Facile Synthesis of Soluble Aromatic Poly(amide amine)s via C–N Coupling Reaction: Characterization, Thermal, and Optical Properties

Guanjun Chang,[1] Li Yang,[1] Junxiao Yang,[1] Yawen Huang,[1] Ke Cao,[1]
Lin Zhang,[2] Runxiong Lin[3]

[1]State Key Laboratory Cultivation Base for Nonmetal Composite and Functional Materials and School of Material Science and Engineering, Southwest University of Science and Technology, Mianyang 621010, People's Republic of China
[2]Joint Laboratory for Extreme Conditions Matter Properties, Southwest University of Science and Technology and Research Center of Laser Fusion, China Academy of Engineering Physics, Mianyang 621900, People's Republic of China
[3]Engineering Research Center of High Performance Polymer and Molding Technology, Ministry of Education, Qingdao University of Science and Technology, Qingdao 266042, People's Republic of China
Correspondence to: G. Chang (E-mail: gjchang@mail.ustc.edu.cn)

Received 23 May 2013; accepted 14 August 2013; published online 10 September 2013
DOI: 10.1002/pola.26910

ABSTRACT: Aromatic poly(amide amine)s (APAAs), as novel high-performance polymers, have been obtained by the condensation polymerization of *N,N′*-bis(4-bromobenzoyl)-*p*-phenylenediamine with two different primary aromatic diamines via palladium-catalyzed aryl amination reaction. The structures of the polymers are characterized by means of FTIR, ^{1}H NMR spectroscopy, and elemental analysis, the results show a good agreement with the proposed structures. DSC and TGA measurements exhibit that polymers possess high glass transition temperature ($T_g > 240$ °C) and good thermal stability with high decomposition temperatures ($T_5 > 400$ °C). These novel polymers also display good solubility. In addition, due to its special structure, APAA-2 is endowed with significantly strong photonic luminescence in *N,N*-dimethylformamide and good electroactivity. © 2013 Wiley Periodicals, Inc. J. Polym. Sci., Part A: Polym. Chem. **2013**, *51*, 4845–4852

KEYWORDS: aromatic poly(amide amine)s; high-performance polymer; palladium-catalysis; soluble; photoluminescence

INTRODUCTION Aramids form a relevant family of polymers that in the past decades have attracted great interest of many research groups, at both the academic and industrial levels, not only as high-performance materials but also for their peculiar conformational and physicochemical behaviors.[1–4] They are finding increasing demand for use as advantageous replacements for metals or ceramics in currently used goods, or even as new materials in novel technological applications.[5–8] In particular, as a type of high-performance polymer, poly(*p*-phenylene terephthalamide) (PPPT) is the earliest, simplest, and best known commercial aramid (Scheme 1). Its transformed materials have applications in advanced coatings, fabrics, and fillers, as advanced composites in the aerospace and armament industry, as asbestos substitutes, electrical insulation, bullet-proof body armor, industrial filters, and protective and sport clothing, among others.[9] However, the extremely high glass transition temperatures of the commercial aramids, which lie above their decomposition temperatures, and their poor solubility in common organic solvents give rise to processing difficulties and limit their applications.[8,9] As a consequence, recent basic and applied research has focused on enhancing their processability and solubility in order to broaden the scope of the technological applications of these materials.[10–13] In addition, there is currently a huge research effort directed toward exploiting the special high performance characteristics of the aramids to obtain electro- or photoluminescent materials, reverse osmosis, gas or ion-exchange membranes, optically active (OA) materials, nanocomposites, and so on with superior thermomechanical performances.[14–17]

The catalytic amination reaction of arylene halides with primary amines using palladium complexes has become an important synthetic procedure for a variety of arylene amines including pharmaceuticals, electronic materials, and ligands for metal catalysts.[18–20] This reaction has become a widely used practical synthetic method for C[sbond]N bond formation. In addition, the Pd-catalyzed aryl amination has also been applied to polycondensation reactions to give various polyamines, poly(imino arylene)s and poly(imino ketone)s with no or scarcely crosslinked structures.[21–25] In this article, the idea is to use Pd-catalyzed aryl amination to synthesize new types of polymers, and two aromatic poly(amide amine)s (APAAs) have been obtained by the polycondensation of

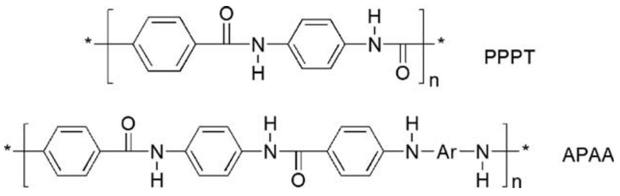

SCHEME 1 The structures of APAA and traditional PPPT.

N,N′-bis(4-bromobenzoyl)-*p*-phenylenediamine with primary aromatic diamines using the catalytic system generated from tris(dibenzylideneacetone)dipalladium (0) $Pd_2(dba)_3$ and 2,2′-bis(diphenylphosphino)-1,1′-binaphthyl (BINAP). The synthesized APAAs can be considered as a hybrid structure of aramids and polyanilines. It is expected that the polycondensation of aramids and polyanilines would result in new soluble polymers (Scheme 1). Functional amine groups on a APAAs backbone also serve as sites for further chemical modification, graft copolymerization, or crosslinking. Furthermore, the Pd-catalyzed aryl amination method provides a facile synthetic route to construct novel structural polymers containing *N*-aryl moieties. Interchain hydrogen bonding, thermal behaviors, solubility, and photoluminescence properties as well as electroactivity of the APAAs are also investigated in detail.

EXPERIMENTAL

Materials

Tris(dibenzylideneacetone)-dipalladium(0) ($Pd_2(dba)_3$) and BINAP were purchased from Alfa Aesar a Johnson Matthey Company in USA. *N,N*′-bis(4-bromobenzoyl)-*p*-phenylenediamine was synthesized in our laboratory. *p*-Phenylenediamine, 4-aminopheyl ether, and sodium *tert*-butoxide were purchased from J & K Technology. The rest materials and reagents were obtained from different commercial sources and used without further purification.

Measurements

FTIR spectra were recorded on a Nicolt 6700 FTIR spectrometer. Elemental analysis was measured on a Vario EL III. ^1H NMR was performed on AVANCE 300 MHz NMR spectrometers in dimethylsulfoxide (DMSO)-d_6. The molecular weights and molecular weight distributions were estimated by gel permeation chromatography (GPC) on a Wyatt DAWN HELEOS using *N*,*N*-dimethylformamide (DMF) (adding 1% LiBr) as an eluent, testing temperature 50 °C. The glass transition temperature was obtained by DSC curves at a rate of 10 °C min^{-1} under flowing nitrogen gas. Thermo gravimetric analysis was performed on a Setarma TG-92 at a heating rate of 10 °C min^{-1} under oxygen and nitrogen atmosphere. Absorption spectra were detected on a SHIMADZU UV-3150 UV–vis–NIR sprectrophotometer. Fluorescent emission spectra were collected on a PerkinElmer LS-55 fluorescence spectrometer. The cyclic voltammograms were obtained with a Zennium IM6 electrochemical workstation (Zahner, Germany) using a normal three-electrode cell with a Pt working electrode, a Pt wire counter electrode, and a Ag/AgCl reference electrode in 1.0 M H_2SO_4 at a scan rate of 20 mV s^{-1}, using ferrocene (with a highest occupied energy molecular orbital (HOMO) energy level, E_{HOMO} = ca. 4.8 eV) as an external standard.

Synthesis of N,N′-Bis(4-bromobenzoyl)-p-phenylenediamine

A three-necked flask equipped with a magnetic stirrer, a condenser and an addition funnel was charged with *p*-phenylenediamine (4.65 g, 0.05 mol), triethylamine (11.11 g, 0.11 mol), and washed with 250 mL of tetrahydrofuran. The 4-bromobenzoyl chloride (24.15 g, 0.11 mol) was added dropwise to the solution (−5 °C) under nitrogen. The precipitate which formed was isolated by filtration and rinsed with both water and methanol to remove salts and excess 4-bromobenzoic acid. Recrystallization of the crude product from *N*-methylpyrrolidone (NMP) afforded *N,N*′-bis(4-bromobenzoyl)-*p*-phenylenediamine as a white crystalline powder.

Yield: 91%; FTIR spectrum (KBr pellet, cm^{-1}): 3308 (N[sbond]H), 1647 (C[dbond]O), 843 (*p*-disubstituted benzene); ^1H NMR (300 MHz, DMSO-d_6): δ = 7.74 (d, J = 8.7 Hz, 8H), 7.90 (d, J = 8.7 Hz, 4H), 10.33 (s, 2H) ppm; ^{13}C NMR (75 MHz, DMSO-d_6): δ = 120.7, 125.2, 129.7, 131.3, 134.0, 134.8, 164.2 ppm; Anal. Calcd. for $C_{20}H_{14}Br_2N_2O_2$ (474.15): C, 50.63; H, 2.95; N, 5.91. Found: C 50.60, H 2.96, N 5.90.

Synthesis of Aromatic Poly(amide amine)s

A typical synthesis of a APAAs was conducted in a three-necked flask (50 mL) equipped with a magnetic stirrer, a nitrogen outlet, inlet, and water-cooled condenser, added to which are *N,N*′-bis(4-bromobenzoyl)-*p*-phenylenediamine (5.0 mmol), primary aromatic diamines (5.0 mmol), sodium *tert*-butoxide (14.0 mmol), tris(dibenzylideneacetone)dipalladium(0) $Pd_2(dba)_3$ (0.05 mmol), BINAP (0.15 mmol), and *N*,*N*-dimethylacetamide (DMAc) (15 mL). The reaction mixture was flushed with high purity nitrogen and the flask was immersed in a 130 °C oil bath for 10–12 h. The resulting polymer solution was allowed to slowly cold to room temperature, filtered, and subsequently poured into methanol, the powder precipitate was filtered, washed with methanol several times, and then dried at 100 °C under vacuum.

APAA-1: Yield: 93%; FTIR spectrum (KBr pellet, cm^{-1}): 3320 (N[sbond]H), 1694 (C[dbond]O), 1306 (C[sbond]N); ^1H NMR (300 MHz, DMSO-d_6): δ = 7.03 (d, J = 8.4 Hz, 4H), 7.18 (s, 4H), 7.71 (m, 4H), 7.85 (d, J = 8.7 Hz, 4H), 8.52 (s, 2H), 9.89 (s, 2H) ppm; Anal. Calcd. for $(C_{26}H_{20}N_4O_2)_n$ $(420.48)_n$: C, 74.28; H, 4.76; N, 13.33; Found: C, 74.16; H, 4.78; N, 13.30.

APAA-2: Yield: 82%; FTIR spectrum (KBr pellet, cm^{-1}): 3317 (N[sbond]H), 1698 (C[dbond]O), 1304 (C[sbond]N); ^1H NMR (300 MHz, DMSO-d_6): δ = 7.00 (t, J = 9.0 Hz, 8H), 7.19 (d, J = 9.0 Hz, 4H), 7.70 (d, J = 7.5 Hz, 4H), 7.85 (d, J = 8.7 Hz, 4H), 8.56 (s, 2H), 9.90 (s, 2H) ppm; Anal. Calcd. for $(C_{32}H_{24}N_4O_3)_n$ $(512.58)_n$: C, 75.00; H, 4.69; N, 10.94; Found: C, 74.92; H, 4.70; N, 10.92.

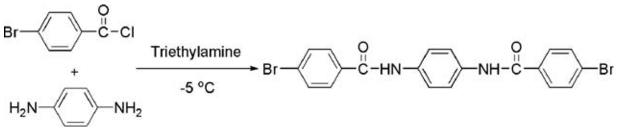

SCHEME 2 Synthesis of *N,N′*-bis(4-bromobenzoyl)-*p*-phenylenediamine.

RESULTS AND DISCUSSION

Design, Synthesis, and Characterization of Polymers

The *N,N′*-bis(4-bromobenzoyl)-*p*-phenylenediamine, as the monomer, was synthesized by the condensation of 4-bromobenzoyl chloride with *p*-phenylenediamine via amidation reaction. The synthetic route to *N,N′*-bis(4-bromobenzoyl)-*p*-phenylenediamine is shown in Scheme 2. The structure of *N,N′*-bis(4-bromobenzoyl)-*p*-phenylenediamine was characterized by FTIR, ^{1}H NMR, and elemental analysis, and the results showed a good agreement with the proposed structure.

The accepted mechanism of the Pd-catalyzed amination involves oxidative addition of the aromatic halides to a palladium(0) species to form an arylene palladium(II) halide. By inductive effect or by resonance, this step should be favored for an arylene bromide substituted with an electron-withdrawing group in the para position. In addition, reactions of electron-deficient aromatic halides and electron-rich amines give high yields in the amination protocol.[20,26] Thus, we attempted to do polycondensation of *N,N′*-bis(4-bromobenzoyl)-*p*-phenylenediamine as electron-poor arylene halides with two different electron-rich primary aromatic diamines (Scheme 3). As expected, the proposed polymers were successfully obtained with high yields and high molecular weights.

The synthesized polymers were characterized by FTIR, ^{1}H NMR, and elemental analysis. The results were in good agreement with the proposed structures. As an example, the ^{1}H NMR spectra of APAA-1 and APAA-2 are shown in Figure 1 (DMSO-d_6). The molecular weights of the reprecipitated polymers were measured by GPC (calibrated by polystyrene standards). The M_n and M_w values are exhibited in Table 1, with increasing molecular weights, the polydispersity increases drastically (Table 1).

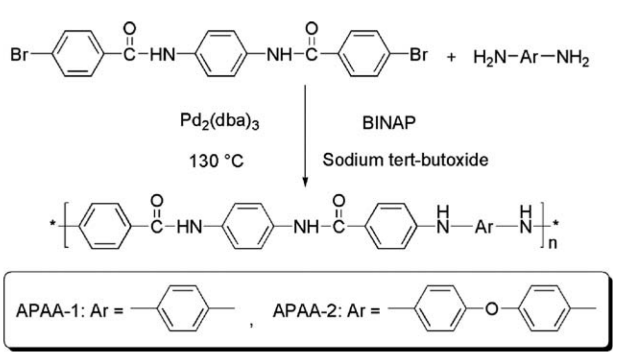

SCHEME 3 Synthesis of aromatic poly(amide amine)s (APAAs) *via* Pd-catalyzed aryl amination.

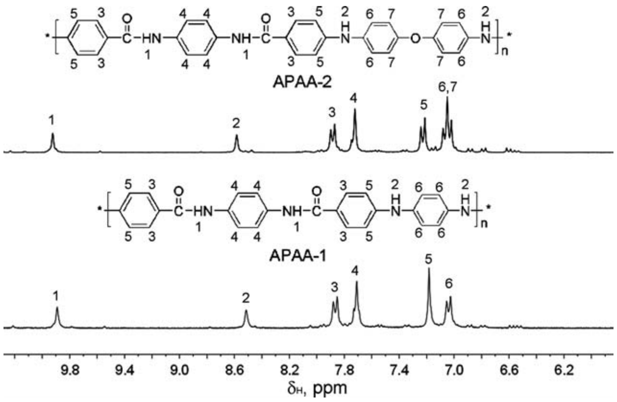

FIGURE 1 ^{1}H NMR (300 MHz) spectra of APAAs recorded in DMSO-d_6.

During the synthesis of polymers, the effect of concentration and temperature on the molecular weight could be followed. Taking APAA-2 as an example, upon increasing the temperature from 70 to 160 °C, M_n and M_w increases at first and then decreases, while upon increasing the concentration from 20 to 35%, M_n and M_w both increased. It is implied in Table 2 that a temperature of 130 °C and a concentration of 35% are more suitable for the palladium-catalyzed polycondensation to produce these polymers with higher molecular weights.

Interchain Hydrogen Bonding

The radial distribution function (RDF) is a useful method in the structural investigation of both solid and liquid packing (local structure) for studying specific interactions such as hydrogen bonding.[27,28] The interactions between the [Sbond]C[dbond]O groups and the [sbond]NH groups in the amide and amine moieties of the APAA can be investigated by means of the RDF, $g_{A\text{-}B}(r)$, where A and B are [sbond]C[dbond]O and [sbond]NH groups, respectively. The inset in Figure 2 displays the RDF of the hydrogen atoms of the amine group (NH) relative to the oxygen atoms of the carbonyl groups (C[dbond]O). It can be observed that the distance between the NH groups and the CO groups of APAA-1 and APAA-2 are about 2.18 and 2.39 Å, respectively, which indicates a strong interaction between these groups. A number of interchain hydrogen bonds are formed. Figure 2 demonstrates the interchain hydrogen-bonding interactions between the [sbond]C[dbond]O and [sbond]NH groups of APAAs.

Moreover, hydrogen-bonding interactions of polymers have frequently been studied by FTIR spectroscopy.[29] Therefore, FTIR of APAAs (KBr pellets) were recorded, giving results to

TABLE 1 Molecular Weights and the Yields of Aromatic Poly (amide amine)s[a]

Polymer Code	M_n	M_w	M_w/M_n	Yield (%)
APAA-1	30,400	98,300	3.23	93
APAA-2	25,500	68,900	2.72	82

[a] The polymer solutions in DMF were calibrated by GPC polystyrene standards.

TABLE 2 Different Experimental Conditions for APAA-2

Run	Temperature (°C)	Concentration of Monomers (%)	M_n	M_w	M_w/M_n	Yield (%)
1	70	15	–[a]	–	–	–
2	100	15	4,200	8,900	2.12	69
3	100	25	9,800	23,100	2.36	79
4	130	35	25,500	68,900	2.70	82
5	160	35	16,800	56,600	3.37	86

[a] –, There is no polymer formed.

corroborate the proposed structures. Typical FTIR spectra at different temperatures are shown in Figure 3. The characteristic absorptions for amine groups υ (NH) appeared between 3318 and 3422 cm^{-1}. Obviously, because of hydrogen bonding, a significant lowering of the absorption frequency of the bands υ (NH) are observed, and the hydrogen-bonding interactions decrease with the temperature increasing. This effect is known to be a function of the degree and strength of the hydrogen bonding.[30] This clearly indicates that N[sbond]H···O[dbond]C interactions from neighboring molecules (Scheme 4). Comparing the frequencies of the NH bond of traditional PPPT (ca. 3300 cm^{-1}),[9] with those observed in the APAAs (ca. 3305 cm^{-1}), a slight shift to higher frequencies is observed. This suggests that the hydrogen bonding in APAAs is weaker than that in PPPT. We assumed that the introduction of amine units gave rise to much more hydrogen donors in polymer chains, in other words, the hydrogen acceptors were relatively decreased, which would further result in lower degree of hydrogen bonds relative to the traditional PPPT.[31]

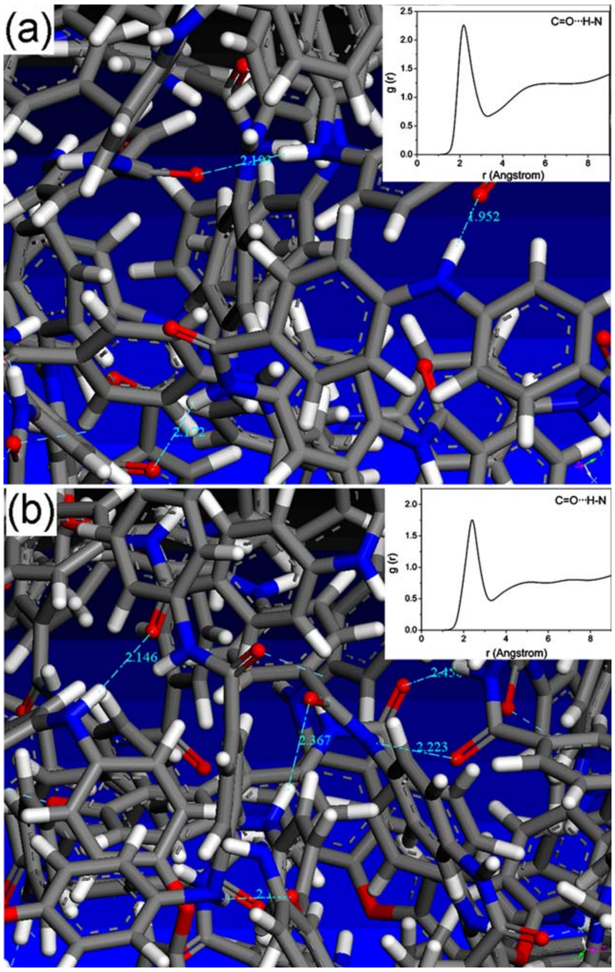

FIGURE 2 Hydrogen bonds between the [sbond]CO[sbond] group and the [sbond]NH[sbond] group of the APAA-1 (a) and the APAA-2 (b). [Color figure can be viewed in the online issue, which is available at wileyonlinelibrary.com.]

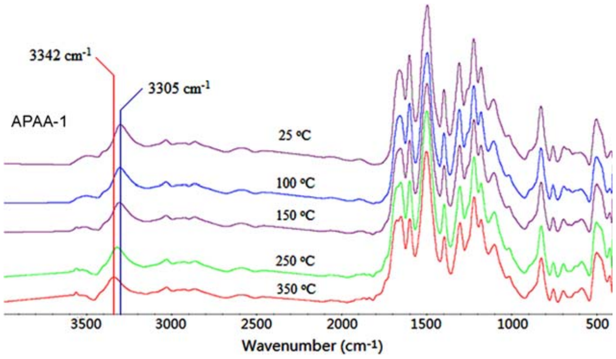

FIGURE 3 FTIR spectra at different temperatures of APAA-1. [Color figure can be viewed in the online issue, which is available at wileyonlinelibrary.com.]

Thermal Behaviors

The thermal properties of APAAs were evaluated via thermogravimetric analysis (TGA) and the data are summarized in Table 3. The synthesized polymers displayed high thermal stability and a high char yield in nitrogen at 800 °C. Typical TGA traces in oxygen and nitrogen are shown in Figure 4 for APAAs. TGA curves revealed that the polymers were thermally stable at up to 400 °C. The 50% weight losses took place at over 800 °C in nitrogen. The APAAs showed higher decomposition temperatures in nitrogen than that in oxygen. Compared with APAA-2, APAA-1 exhibited better thermal stability. Char yield is an easy and important measurement which correlates to the ability to sustain combustion. For

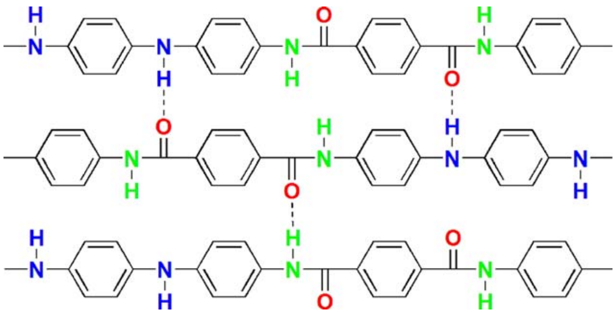

SCHEME 4 The hydrogen-bonding interactions of aromatic poly(amide amine)s. [Color figure can be viewed in the online issue, which is available at wileyonlinelibrary.com.]

TABLE 3 Thermal Analysis Data for APAAs

Polymer Code	O_2/N_2	T_5[a]	T_{10}[b]	T_{50}[c]	Char Yield at 800 °C[d]
APAA-1	O_2	502	550	783	31
	N_2	570	598	>800	67
APAA-2	O_2	461	529	775	25
	N_2	528	568	>800	57

[a] T_5: temperature of 5% weight loss.
[b] T_{10}: temperature of 10% weight loss.
[c] T_{50}: temperature of 50% weight loss.
[d] The remaining of the polymer at 800 °C.

these two polymers, the char yield in nitrogen at 800 °C was up to 57% (Table 3).

Differential scanning calorimetry (DSC) of these polymers up to 250 °C exhibited a single T_g. Two representative DSC thermograms of the polymers are shown in Figure 5. The polymers displayed high T_gs ranging from 248 to 275 °C. The T_gs are higher than those of the related poly(ether ketone)s (PEKs) which range from 129 to 167 °C and lower than those of aramids which amount to 292–319 °C. Moreover, APAA-1 also displayed a visible melting temperature T_m (350 °C). While the observed T_m value is significantly lower than that of PPPT (T_m = 570 °C) and slightly higher than that of poly(ether ether ketone) (PEEK), which has a T_m of 343 °C.[32] This can be explained by the hydrogen bonding in APAAs which is weaker than that in aramids while PEKs have no hydrogen bonding.

Wide-Angle X-Ray Diffraction

The crystallization characteristic of the PPPT results from its chemical structure. The wholly aromatic structure with all-para substitutions creates stiff rod-like macromolecules, having a high cohesive energy and a high crystallization tendency due to the very favorable intramolecular hydrogen bonds.[9] Compared with the structure of PPPT, the amine groups were introduced in the polymer chain, and the novel APAAs were obtained. The wide-angle X-ray diffraction patterns of the polymers over the 2θ range of 5-30° are displayed in Figure 6. Polymer APAA-1 exhibited the most noticeable diffractions peaks at 2θ = 12.6° (A, d = 7.0 Å),

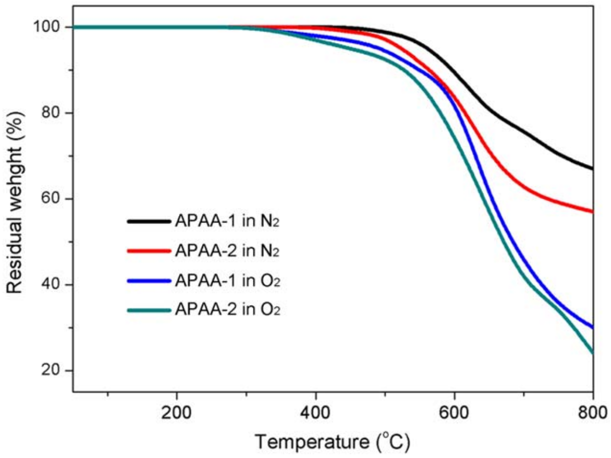

FIGURE 4 TGA curves of aromatic poly(amide amine)s in oxygen and nitrogen. [Color figure can be viewed in the online issue, which is available at wileyonlinelibrary.com.]

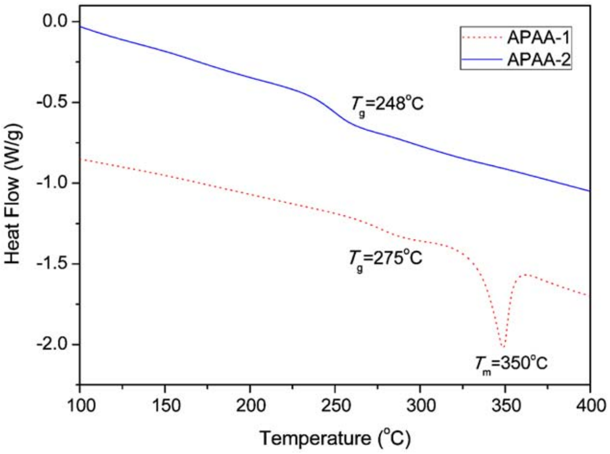

FIGURE 5 DSC curves of aromatic poly(amide amine)s in nitrogen. [Color figure can be viewed in the online issue, which is available at wileyonlinelibrary.com.]

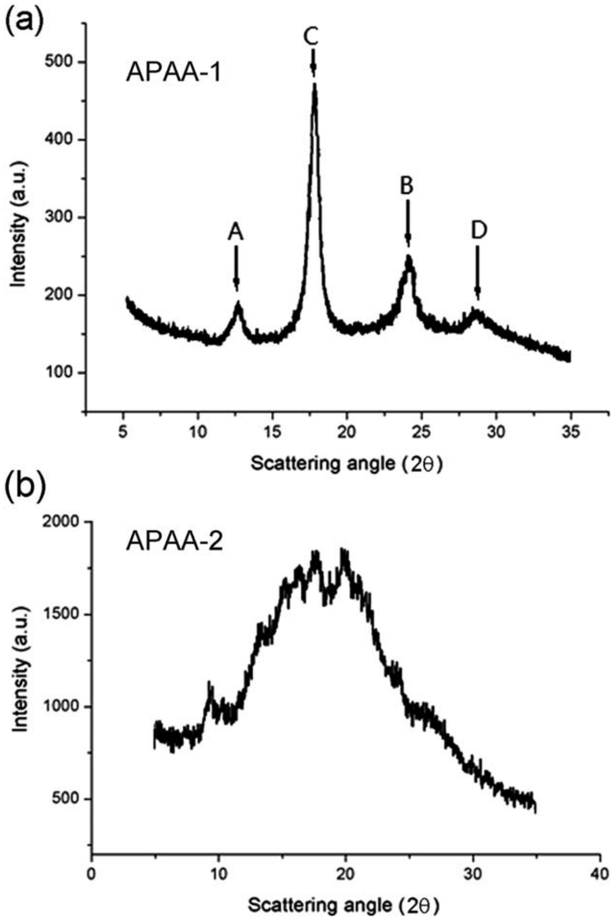

FIGURE 6 WAXD diffractograms intensity versus Bragg angle graph for (a) APAA-1 and (b) APAA-2.

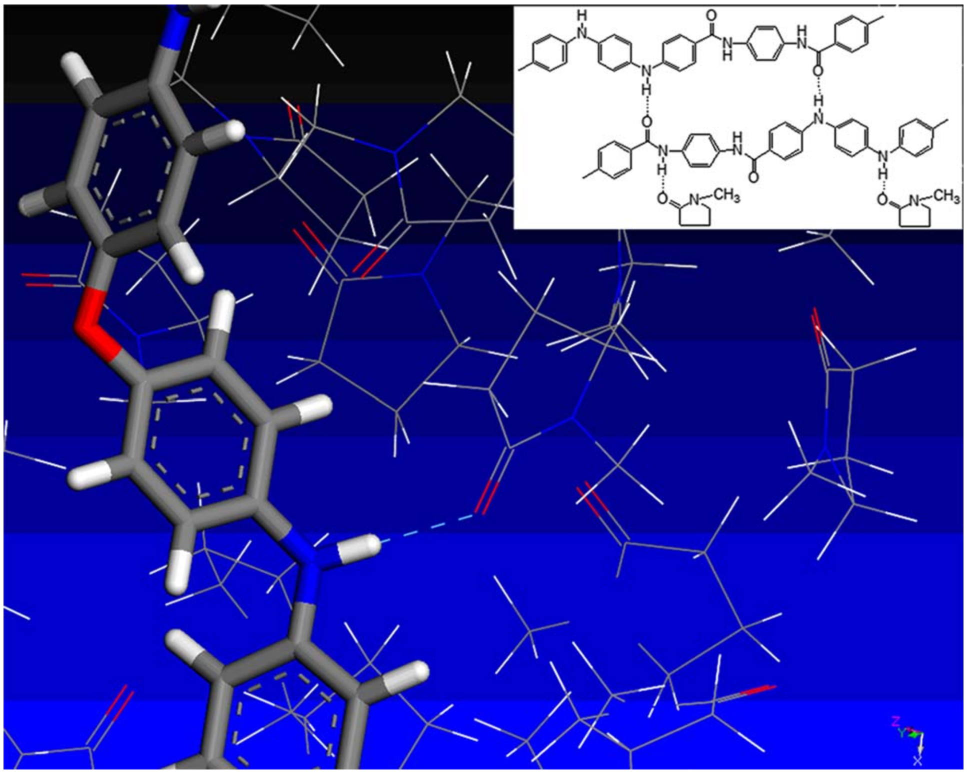

FIGURE 7 Hydrogen bonding between solvent and APAA. [Color figure can be viewed in the online issue, which is available at wileyonlinelibrary.com.]

18.0° (C, $d = 4.8$ Å), 24.4° (B, $d = 7.0$ Å), and 28.9° (D, $d = 3.0$ Å), which are quite similar to the (200), (110), (200), and (211) reflections [Figure 6(a)]. The reflection B in the scattering pattern is exactly in a double distance on the scattering vector coordinates as A and can be considered as a second-order one but related to the same correlation period as A.[33,34] Obviously, the ether groups hindered chain packing and reduced the level of ordering, thus leading to the amorphous nature of APAA-2 ([Figure 6(b)]. The amorphous nature of APAA-2 was also reflected in its good solubility. By comparing WAXD of APAA-2 with APAA-1, the latter polymer exhibited semicrystalline behavior, and we can conclude that insertion of ether group groups into the repeating units of the polymers resulted in a significant increase of the amorphous nature of the polymer.

Solubility

The APAAs can be considered as hybrid structure of aramids and polyaniline. It was expected that the combination of aramids and polyaniline would result in improved solubility. In addition, the hydrogen bonding between solvent and the APAAs could be formed, which has been proved by molecular simulation (Figure 7). Because of their hydrogen bonding interactions, APAAs demonstrated good solubility in most organic solvents.

These novel polymers showed different solubility behavior in different organic solvents. Polymer solubility was qualitatively determined by the dissolution of 5 mg of solid polymers in 1 mL of organic solvents at room temperature and 50 °C (Table 4). The polymers could be easily soluble in high polar solvents, such as DMAc, DMSO, NMP, and DMF. By comparing APAA-1 with APAA-2, the latter polymer exhibited better solubility, and this was reflected in its amorphous nature. The two APAAs both showed improved solubility compared with aramids.[9]

Optical and Photoluminescence Properties

Light-emitting phenomenon is a characteristic of luminescence materials. Outstanding luminescence properties of aramids make these polymers suitable for the production of specifically polymer light-emitting diodes (PLEDs). There is currently much research directed toward the preparation of blue light-emitting polymers, because blue light can be converted to green or red using the proper dyes, which means a blue PLED alone is capable of generating all colors, while green or red cannot emit blue light by this method. In this article, the UV spectra of APAA-1 and APAA-2 were first investigated in DMF. As displayed in Figure 8(a), the two

TABLE 4 Solubility of Polymers

Polymer Code	DMAc	DMSO	DMF	NMP	$CHCl_3$
APAA-1	+ +[a]	+ +	+ –[b]	+ +	+ –
APAA-2	+ +	+ +	+ +	+ +	+ +

[a] + +, Solid polymer was completely dissolved at room temperature.
[b] + –, Solid polymer was completely dissolved at 50 °C.

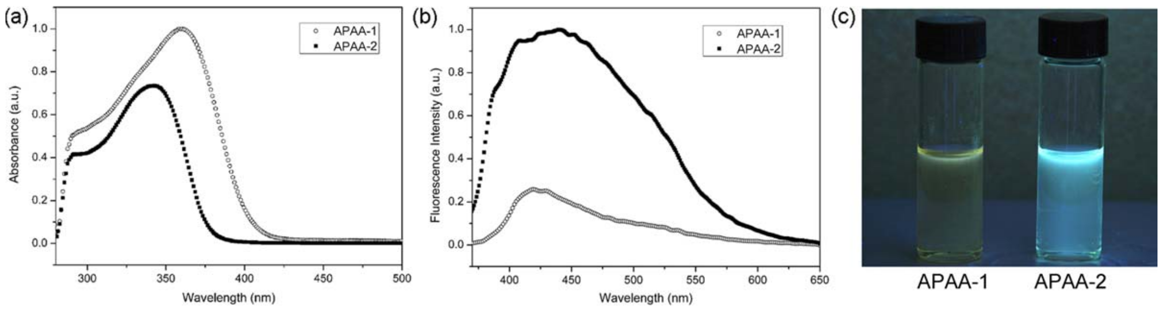

FIGURE 8 (a) Overlay of the absorbance curves of APAA-1 and APAA-2. (b) Fluorescence spectra of APAA-1 and APAA-2 in DMF (λ_{exc} = 360 nm; excitation and emission slits = 5.0 and 5.0 nm, respectively). (c) Fluorescence images of APAA-1 and APAA-2 (λ_{exc} = 365 nm) in DMF. [Color figure can be viewed in the online issue, which is available at wileyonlinelibrary.com.]

polymers gave rise to similar UV absorption bands. However, the long wavelength absorption maximum (359 nm) of APAA-1 was 16-nm bathochromic shift compared with that of APAA-2, implying that the relative flexible ether group structure of APAA-2 might freely rotate in the polymer chains and thus restrict the conjugation of the pheny unit. Moreover, we found that APAA-2 exhibited significantly strong photonic luminescence in DMF [Figure 8(c)]. As shown in Figure 8(b), the emission maximum of APAA-2 at 440 nm was bathochromic shift relative to that of APAA-1 (420 nm) with a dramatic increase in intensity. The fluorescence quantum yields (Φ_F) of APAA-1 and APAA-2 determined in DMF solutions using quinine sulfate (Φ_F = 55% in 1 M H_2SO_4) as standard are 7.5 and 34.2%, respectively.[2] It is suggested that the intensity of the photonic emission is heavily depend upon the structures of the polymers. As compared to APAA-1, there is a "push-pull" π-electron mode in APAA-2, in which the oxygen atom of the ether moiety serves as the electron donor and the electron-deficient groups of amide act as the electron acceptor. Hence, the polymer will undergo an intramolecular charge transfer from the donor to the acceptor upon excitation by light.

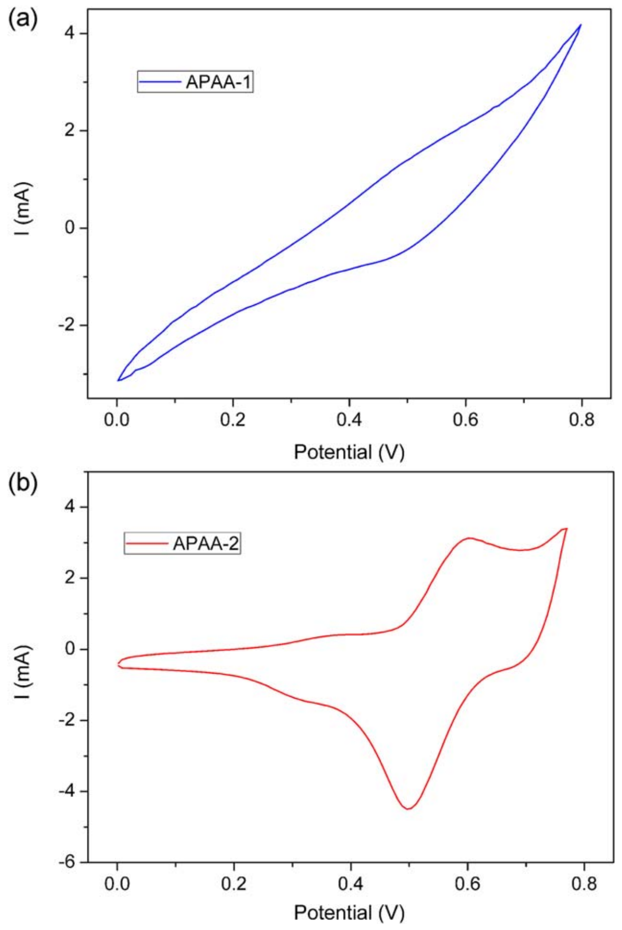

FIGURE 9 CV measurements of (a) APAA-1 and (b) APAA-2 conducted in aqueous H_2SO_4 (1.0 M) at a scan rate of 20 mV s^{-1}. [Color figure can be viewed in the online issue, which is available at wileyonlinelibrary.com.]

The energy levels of the HOMO and LUMO were determined by measuring the electrochemical properties of the polymers using cyclic voltammetry (CV) with a standard three-electrode. A platinum (Pt) electrode was modified with a polymer film by means of dip-coating, and was used as the working electrode. A Pt wire was used as the counter electrode, and Ag/AgCl (4.0 M KCl) served as the reference electrode. The CV measurements were carried out in a 1.0 M H_2SO_4 electrolyte at room temperature at a scan rate of 20 mV s^{-1}. The scanned cyclic voltammograms are shown in Figure 9. The redox process of APAA-1 was very weak under our experimental conditions [Figure 9(a)]. In contrast, the

TABLE 5 Electrochemical Data of Polymers

Polymer Code	λ_{onset} (nm)	E_g[a] (eV)	E_{onset} (eV)	HOMO[b] (eV)	LUMO[c] (eV)
APAA-1	420	2.95	–[d]	–	–
APAA-2	385	3.22	0.48	–5.28	–2.06

[a] Optical band gap calculated from the UV–Vis absorption onset.

[b] The HOMO energy levels were calculated from cyclic voltammetry and were referenced to ferrocene (4.8 eV).

[c] LUMO levels of the polymer were estimated from the optical band gaps and the HOMO energies.

[d] Not measured due to weak signals.

oxidation process of APAA-2 had an onset at 0.48 V and gave a peak at 0.60 V. The oxidation was pseudoreversible and gave the corresponding reduction peak at 0.50 V. The energy levels of the HOMO and the LUMO were thus estimated from the cyclic voltammograms and the onset of the absorption spectra. The results are summarized in Table 5. The APAA-2 has relatively lower energy levels, which means that a better hole transporting ability can be expected.[35]

CONCLUSIONS

Two novel APAAs have been successfully synthesized by a Pd-catalyzed polycondensation of *N,N'*-bis(4-bromobenzoyl)-*p*-phenylenediamine with different primary aromatic amines. These polymers can be considered as a new class of high-performance polymers with high thermal stability ($T_g > 240$ °C and $T_5 > 400$ °C). Their good solubilities broaden the scope of the technological applications of these materials. Moreover, APAA-2 displays significantly strong photonic luminescence in DMF and good electroactivity, which warrants its potential applications for photoluminescent devices. This work does not only deepen our systemic understanding of the synthetic strategy of Pd-catalyzed polycondensation but also provide new perspectives for generating polymers with thermal stability, good solubility, and well optical properties.

ACKNOWLEDGMENTS

This research was financially supported by the National Natural Science Foundation of China (No. 21202134), the Research Fund for the Doctoral Program of Southwest University of Science and Technology (No. 12zx7129), Science and Technology Development Foundation of China Academy of Physics Engineering (Nos. 2012A0302015 and 2012B0302050).

REFERENCES AND NOTES

1 J. K. Fink, High Performance Polymers; William Andrew: New York, **2008**.

2 G.-S. Liou, C.-W. Chang, *Macromolecules* **2008**, *41*, 1667–1674.

3 J. Gallini, In Encyclopedia of Polymer Science and Technology; Wiley: New York, **2005**; Vol. *3*, p 558.

4 M. Laurati, P. Sotta, D. R. Long, L.-A. Fillot, A. Arbe, A. Alegrìa, J. P. Embs, T. Unruh, G. J. Schneider, J. Colmenero, *Macromolecules* **2012**, *45*, 1676–1687.

5 S. Mallakpour, Z. Rafiee, *Amino Acids* **2009**, *37*, 665–672.

6 S. Cakir, M. Nieuwenhuizen, P. G. A. Janssen, R. Rulkens, C. E. Koning, *Polymer* **2012**, *53*, 5242–5250.

7 Y. Jin, Z. Su, *J. Membr. Sci.* **2009**, *330*, 175–179.

8 A. Arun, K. Dullaert, R. J. Gaymans, *Macromol. Chem. Phys.* **2009**, *210*, 48–59.

9 J. M. García, F. C. García, F. Serna, J. L. de la Peña, *Prog. Polym. Sci.* **2010**, *35*, 623–686.

10 M. Ghaemy, H. Behmadi, R. Alizadeh, *Chin. Chem. Lett.* **2009**, *20*, 961–964.

11 S. R. Sheng, X. L. Pei, Z. Z. Huang, X. L. Liu, C. S. Song, *Eur. Polym. J.* **2009**, *45*, 230–236.

12 A. Shockravi, E. Abouzari-Lotf, S. Taheri, *Polym. J.* **2009**, *41*, 174–180.

13 G. Huang, S. Zhang, D. Li, M. Zhang, G. Zhang, J. Yang, *Polym. Int.* **2013**, *62*, 411–418.

14 D. Y. Kim, H. N. Cho, C. Y. Ki, *Prog. Polym. Sci.* **2000**, *25*, 1089–1139.

15 L. Akcelrud, *Prog. Polym. Sci.* **2003**, *28*, 875–962.

16 G. S. Liou, K. H. Lin, *J. Polym. Sci. Part A: Polym. Chem.* **2009**, *47*, 1988–2001.

17 G. S. Liou, S. H. Hsiao, N. K. Huang, Y. L. Yang, *Macromolecules* **2006**, *39*, 5337–5346.

18 R. Yamasaki, H. Ikeda, H. Masu, I. Azumaya, S. Saito, *Tetrahedron* **2012**, *68*, 8450–8456.

19 J. Ruan, O. Saidi, J. A. Iggo, J. Xiao, *J. Am. Chem. Soc.* **2008**, *130*, 10510–10511.

20 D. S. Surry, S. L. Buchwald, *Chem. Sci.* **2011**, *2*, 27–50.

21 T. Kanbara, S. Takase, K. Izumi, S. Kagaya, K. Hasegawa, *Macromolecules* **2000**, *33*, 657–659.

22 B.-J. Jung, J.-I. Lee, H. Y. Chu, L.-M. Do, H.-K. Shim, *Macromolecules* **2002**, *35*, 2282–2287.

23 A. S. Al-Hussaini, M. Klapper, T. Pakula, K. Müllen, *Macromolecules* **2004**, *37*, 8269–8277.

24 G. Chang, X. Luo, L. Zhang, R. Lin, *Macromolecules* **2007**, *40*, 8625–8630.

25 G. Chang, X. Luo, Y. Xu, H. Hu, L. Wei, L. Zhang, R. Lin, *Polym. Bull.* **2012**, *68*, 95–111.

26 D. Maiti, B. P. Fors, J. L. Henderson, Y. Nakamura, S. L. Buchwald, *Chem. Sci.* **2011**, *2*, 57–68.

27 G. D. Smith, D. Bedrov, O. Borodin, *Phys. Rev. Lett.* **2000**, *85*, 5583–5586.

28 F. Pan, F. Peng, Z. Jiang, *Chem. Eng. Sci.* **2007**, *62*, 703–710.

29 S. Jeon, J. Choo, D. Sohn, S. N. Lee, *Polymer* **2001**, *42*, 9915–9920.

30 J. C. Alvarez, J. G. de la Campa, A. E. Lozano, J. de Abajo, *Macromol. Chem. Phys.* **2001**, *202*, 3142–3148.

31 J. R. Fried, Polymer Science and Technology; Prentice Hall, Upper Saddle River: New Jersey, **2003**.

32 A. E. Lozano, J. de Abajo, J. G. de la Campa, J. Preston, *J. Polym. Sci. Part A: Polym. Chem.* **1995**, *33*, 1987–1994.

33 T. H. Lee, K. Do, Y. W. Lee, S. S. Jeon, C. Kim, J. Ko, S. S. Im, *J. Mater. Chem.* **2012**, *22*, 21624–21629.

34 A. Fortney, E. Fossum, *Polymer* **2012**, *53*, 2327–2333.

35 C. Xia, R. C. Advincula, *Macromolecules* **2001**, *34*, 5854–5859.